Performance Analysis of Coherent FSO System with SSC Receiver

Milica I. Petković[1], Goran T. Đorđević[1]

Abstract: This paper analyzes the performance of coherent free-space optical (FSO) system employing the switch-and-stay (SSC) dual diversity receiver. The intensity fluctuations of the optical signal are modeled by Gamma-Gamma distribution, being caused by atmospheric turbulence. In addition, pointing errors are taken into account. Novel analytical expressions for the outage probability are derived. The general scenario of unbalanced average signal-to-noise ratios (SNRs) of independent and identically distributed SSC branches is considered, which is further simplified to the balanced SNR case. The effects of various system and channel parameters are investigated and discussed.

Keywords: Atmospheric turbulence, Free-space optical (FSO) systems, Outage probability, Pointing errors, Switch-and-stay (SSC) diversity.

1 Introduction

As new rewarding modern technology, free-space optics (FSO) has received a notable research attention. Many advantages, such as high data rate capacity, license-free and low-cost optical wireless transmission, are the reason for the FSO systems to be adopted as the "last mile" solution being alternative or complementary technology to already existing radio frequency networks [1 − 4]. The main reasons of optical signal degradation, during transmission via atmospheric channel, are atmospheric turbulence and pointing errors. The variations in atmospheric temperature and pressure lead to the atmospheric turbulence, i.e., optical signal intensity fluctuations, which are modeled by Gamma-Gamma distribution [2 − 4]. The pointing error or misalignment fading occurs due to poor alignment of the FSO transmitter laser and receiver detector [5 − 9]. In this paper, we adopt statistical model proposed in [5] to describe the effect of pointing errors, when the size of the receiver detector is not neglected. It is assumed that the both horizontal and vertical displacements are modeled by independent identical Gaussian distributions [5]. The final probability density function (PDF) of the optical signal intensity, when both Gamma-Gamma atmospheric turbulence and pointing errors are considered, is presented in [7].

---
[1]Faculty of Electronic Engineering, University of Niš, 14 Aleksandra Medvedeva, 18000 Niš, Serbia;
E-mails: milica.petkovic@elfak.ni.ac.rs; goran@elfak.ni.ac.rs.

As a method to mitigate the optical signal degradation due to mentioned phenomena, the spatial diversity techniques at the transmitter and/or receiver of the FSO system were proposed. The performance of the FSO system employing selection combining (SC), equal gain combining (EGC) or maximum ratio combining (MRC) was observed in [10, 11], assuming weak and strong atmospheric turbulence conditions, respectively. Multiple–input multiple–output FSO system influenced by Gamma–Gamma atmospheric turbulence was observed in [12]. Due to the ability to monitor and process only one diversity branch, the switched combining has received an attention as technique simpler for implementation [13]. In [14], the FSO signal transmission over log-normal atmospheric turbulence channel was observed, when the switch-and-stay combining (SSC) or switch-and-examine (SEC) combining at the reception was employed. The FSO system performance with SSC diversity receiver, when the intensity fluctuations are modeled by Gamma-Gamma distribution was analyzed in [15], while the pointing errors were taken into account in [16].

Aforementioned works relating SSC assumed direct detection at the receiver part of the system. Inspired by mentioned studies above, in this paper we analyze the performance of FSO system with coherent detection, which employs dual-branch SSC receiving aperture. Both Gamma-Gamma atmospheric turbulence and pointing errors are taken into consideration. The assumption that FSO branches are at the adequate distance is adopted, so the correlation between optical beams is not present. The outage expressions are derived, for both unbalanced and balanced average signal-to-noise (SNR) scenarios of independent and identically distributed (i.i.d.) SSC branches.

The rest of the paper is organized as follows. Section II describes the system and channel model. The outage probability analysis is presented in Section III. Numerical results with discussions are given in Section IV. Section V presents some concluding remarks.

2   System and Channel Model

We consider the FSO system with dual-branch SSC diversity, while coherent detection is assumed at each receiver. The FSO systems with coherent detection refer to the systems with the local oscillator, which generates the optical wave that will be added to the received optical signal [3, 17].

The instantaneous SNR, γ_i, for each branch can be defined as [17, (2)]

$$\gamma_i = \frac{\Re A_i I_i}{q \Delta f}, \quad i = 1, 2, \tag{1}$$

where $\Re$ represents each detector responsivity, A_i represents area of the each photodetector, I_i is the normalized irradiance of the *i*-th branch, *q* denotes the

electronic charge, and Δf is the noise equivalent bandwidth of receiver. The average SNR, $\overline{\gamma}_i$, for each branch is defined as [17, (7)]

$$\overline{\gamma}_i = \frac{\Re A_i \mathrm{E}[I_i]}{q \Delta f}, \quad i = 1, 2, \tag{2}$$

where $\mathrm{E}[\cdot]$ represents the mathematical expectation.

The optical signal intensity fluctuations are caused by the Gamma-Gamma atmospheric turbulence, pointing errors and path loss. In this scenario, the optical signal irradiance of the i-th branch is $I_i = I_l I_a I_p$, where I_l is the propagation path loss, I_a defines an attenuation due to atmospheric turbulence, I_p represents an attenuation due to pointing errors. The intensity fluctuations due to atmospheric turbulence are modeled by the Gamma-Gamma distribution, with the PDF of I_a found in [7]. For describing the pointing errors effect, we use model which was proposed by Farid and Hranilovic in [5], and the final closed-form PDF of I_p is given in [7]. The path loss represents deterministic component determined as $I_l = \exp(-\sigma L)$, where σ is the atmospheric attenuation coefficient and L is the propagation distance. If all mentioned FSO channel components are taken into account, the final PDF of I_i is defined as [7, (12)]

$$f_{I_i}(I_i) = \frac{\xi^2 \alpha \beta}{A_0 I_l \Gamma(\alpha) \Gamma(\beta)} G_{1,3}^{3,0}\left(\frac{\alpha\beta}{A_0 I_l} I_i \,\middle|\, \begin{matrix} \xi^2 \\ \xi^2 - 1, & \alpha - 1, & \beta - 1 \end{matrix}\right), \quad i = 1, 2, \tag{3}$$

where $\Gamma(\cdot)$ is the gamma function [18, (8.310.1)] and $G_{p,q}^{m,n}(\cdot)$ is Meijer's G-function [18, (9.301)]. The parameters α and β are related to the atmospheric turbulence, and represent the effective numbers of small-scale and large-scale cells of the scattering environment, respectively, while the parameters ξ and A_0 are related to the pointing errors effect. The parameters α, β, ξ and A_0 will be defined in continuation.

The parameters α and β are the Gamma-Gamma atmospheric turbulence parameters, which are determined as

$$\alpha = \left(\exp\left[0.49\sigma_R^2\middle/\left(1 + 1.11\sigma_R^{12/5}\right)^{7/6}\right] - 1\right)^{-1}, \tag{4}$$

$$\beta = \left(\exp\left[0.51\sigma_R^2\middle/\left(1 + 0.69\sigma_R^{12/5}\right)^{5/6}\right] - 1\right)^{-1}, \tag{5}$$

for the plane wave propagation and zero inner scale. They are dependent on the Rytov variance, which is defined as

$$\sigma_R^2 = 1.23 C_n^2 k^{7/6} L^{11/6}, \tag{6}$$

where $k = 2\pi/\lambda$ is the wave number with the wavelength λ, and C_n^2 represents the refractive index structure parameter, which determines the atmospheric turbulence strength.

The parameter ξ in (3) is related to the pointing errors effect, and it is defined as

$$\xi = \frac{w_{L_{eq}}}{2\sigma_s}, \tag{7}$$

where the pointing error (jitter) standard deviation at the receiver is denoted by σ_s. The equivalent beam waist at the receiver in (7), which is denoted by $w_{L_{eq}}$, is dependent on the beam waist at the distance L, denoted by w_L, as follows

$$w_{L_{eq}}^2 = \frac{w_L^2 \sqrt{\pi} \operatorname{erf}(v)}{2v \exp(-v^2)}, \tag{8}$$

where $v = \sqrt{\pi} a / (\sqrt{2} w_L)$, and a is a radius of circular detector aperture. The parameter A_0 in (3) is defined as $A_0 = \operatorname{erf}^2(v)$, where $\operatorname{erf}(\cdot)$ is the error function [18, (8.250.1)]. Further, the parameter w_L in (8) is in relation with the optical beam radius at the waist, denoted by w_0, as

$$w_L = w_0 \sqrt{(\Theta_o + \Lambda_o)(1 + 1.63\sigma_R^{12/5}\Lambda_1)}, \tag{9}$$

where $\Theta_o = 1 - L/F_0$, $\Lambda_o = 2L/(kw_0^2)$, $\Lambda_1 = \Lambda_o/(\Theta_o^2 + \Lambda_o^2)$, and F_0 represents the radius of curvature [8].

Based on (3), it is obtained that $\mathrm{E}[I_i] = A_0 I_l \xi^2 / (\xi^2 + 1)$. Therefore, based on (2), the average SNR, $\overline{\gamma}_i$, for each branch is derived as

$$\overline{\gamma}_i = \frac{\Re A_i \mathrm{E}[I_i]}{q\Delta f} = \frac{\Re A_i}{q\Delta f} \frac{A_0 I_l \xi^2}{\xi^2 + 1} = \frac{\Re A_i}{q\Delta f} A_0 I_l \kappa, \quad i = 1, 2, \tag{10}$$

where $\kappa = \xi^2 / (\xi^2 + 1)$. Based on (1) and (3), after applying standard technique of transforming random variables, $f_{\gamma_i}(\gamma_i) = f_{I_i}(I_i) / |\partial \gamma_i / \partial I_i| \Big|_{I_i = \frac{\gamma_i}{\overline{\gamma}_i} A_0 I_l \kappa}$, and some mathematical manipulations, the PDF of γ_i is derived as

$$f_{\gamma_i}(\gamma_i) = \frac{\xi^2 \alpha\beta\kappa}{\Gamma(\alpha)\Gamma(\beta)\overline{\gamma}_i} G_{1,3}^{3,0}\left(\alpha\beta\kappa\frac{\gamma_i}{\overline{\gamma}_i} \middle| \begin{matrix} \xi^2 \\ \xi^2-1, \quad \alpha-1, \quad \beta-1 \end{matrix} \right), \quad i=1,2. \quad (11)$$

After utilizing [19, (07.34.16.0001.01)] to reduce the order of Meijer's G-function in (11), the PDF of γ_i is found as [20]

$$f_{\gamma_i}(\gamma_i) = \frac{\xi^2}{\Gamma(\alpha)\Gamma(\beta)\gamma_i} G_{1,3}^{3,0}\left(\alpha\beta\kappa\frac{\gamma_i}{\overline{\gamma}_i} \middle| \begin{matrix} \xi^2+1 \\ \xi^2, \quad \alpha, \quad \beta \end{matrix} \right), \quad i=1,2. \quad (12)$$

The cumulative distribution function (CDF) of γ_i is found by applying [19, (07.34.21.0084.01)] as

$$F_{\gamma_i}(x) = \frac{\xi^2}{\Gamma(\alpha)\Gamma(\beta)} G_{2,4}^{3,1}\left(\alpha\beta\kappa\frac{x}{\overline{\gamma}_i} \middle| \begin{matrix} 1, \quad \xi^2+1 \\ \xi^2, \quad \alpha, \quad \beta, \quad 0 \end{matrix} \right), \quad i=1,2. \quad (13)$$

3   Outage Probability Analysis

This section presents an analysis of the observed system outage probability. We assume that dual-branch SSC diversity is applied at the receiver, so the outage probability is determined as the probability that the instantaneous SNR at SSC output, denoted by γ_{SSC}, falls below a predetermined outage threshold, denoted by q. Besides general unbalanced SNR scenario, we also present the analysis of the simpler balanced SNR scenario.

3.1 Unbalanced SNR scenario

The outage probability of the system under investigation, when unbalanced SNR scenario is considered, represents the CDF of the instantaneous SNR at SSC output, γ_{SSC}. By denoting the switching threshold as γ_T, the CDF of γ_{SSC} is determined as [21]

$$F_{ssc}(\gamma) = \begin{cases} \dfrac{F_1 F_2}{F_1+F_2} \displaystyle\sum_{i=1}^{2} F_{\gamma_i}(\gamma), & 0 < \gamma \le \gamma_T, \\[3mm] \dfrac{F_1 F_2}{F_1+F_2} \displaystyle\sum_{i=1}^{2}\left(F_{\gamma_i}(\gamma) + \dfrac{F_{\gamma_i}(\gamma)}{F_i} - 1 \right), & \gamma > \gamma_T, \end{cases} \quad (14)$$

where $F_{\gamma_i}(\gamma)$ is defined by (13), while $F_i, (i=1,2)$, is

$$F_i = F_{\gamma_i}(\gamma_T), \quad i=1,2. \quad (15)$$

Finally, the outage probability for unbalanced SNR scenario is found as

$$P_{out} = F_{ssc}(q). \quad (16)$$

3.2 Balanced SNR scenario

Under the assumption that the average SNRs of each branch are equal, i.e., $\overline{\gamma}_1 = \overline{\gamma}_2$, the simpler balanced SNR scenario is observed. In this case, the PDFs and CDFs of the instantaneous SNRs for each branch are equal, meaning $f_{\gamma_1}(\gamma) = f_{\gamma_2}(\gamma) = f_\gamma(\gamma)$ and $F_{\gamma_1}(\gamma) = F_{\gamma_2}(\gamma) = F_\gamma(\gamma)$. Based on (14), the CDF of γ_{SSC} is found as [21]

$$F_{ssc}^b(\gamma) = \begin{cases} F_\gamma(\gamma_T) F_\gamma(\gamma), & 0 < \gamma \leq \gamma_T \\ F_\gamma(\gamma_T)\left(F_\gamma(\gamma) + \dfrac{F_\gamma(\gamma)}{F_\gamma(\gamma_T)} - 1 \right), & \gamma > \gamma_T \end{cases} \quad . \tag{17}$$

The outage probability for balanced SNR scenario is can be easily found as

$$P_{out} = F_{ssc}^b(q). \tag{18}$$

4   Numerical Results

This section presents the numerical results obtained based on derived outage probability expressions in (16) and (18). The atmospheric turbulence strength is defined by the index of refraction structure parameter as: $C_n^2 = 6 \times 10^{-15} \text{ m}^{-2/3}$ in weak, $C_n^2 = 2 \times 10^{-14} \text{ m}^{-2/3}$ in moderate, and $C_n^2 = 5 \times 10^{-14} \text{ m}^{-2/3}$ in strong conditions of the atmospheric turbulence. The wavelength takes a value of $\lambda = 1550$ nm, and the radius of the circular detector aperture is $a = 5$ cm. Radius of curvature is $F_0 = -10$ m [8].
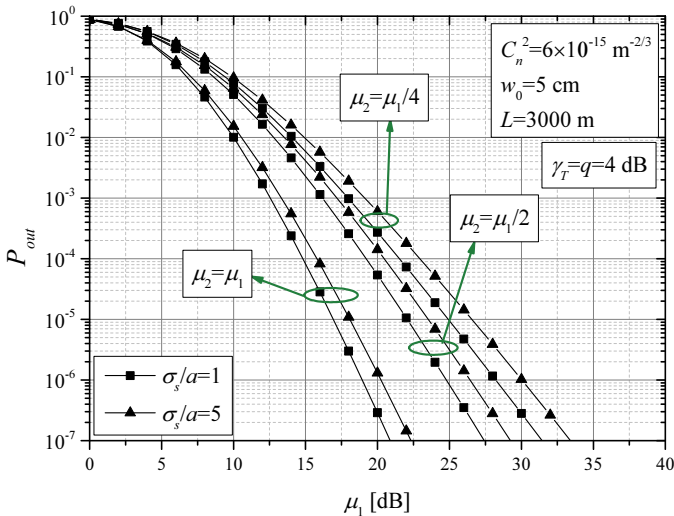

Fig. 1 – *Outage probability versus* μ_1 *for unbalanced SNR scenario.*

Fig. 1 shows the outage probability dependence on the average SNR, μ_1, for unbalanced SNR scenario, assuming different values of the normalized jitter standard deviation. When branch unbalancing occurs, the increase of outage probability degradation is present. Hence, the best system performance is achieved when $\mu_1 = \mu_2$, corresponding to the balanced SNR scenario when signals at the receiver are with equal powers. Furthermore, it can be concluded that lower value of the normalized jitter standard deviation results in better system performance. When the normalized jitter standard deviation takes a lower value, the positioning of the FSO transmitter laser and receiver photodetector is better, and the pointing errors effect is less expressed. Furthermore, it is observed that the degradation due to the SSC branch unbalancing is not dependent on the pointing errors strength.
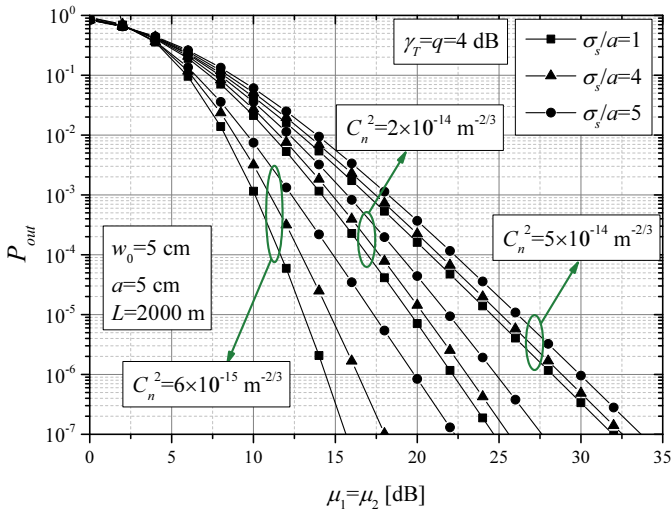

Fig. 2 – *Outage probability versus* $\mu_1 = \mu_2$ *for different values of normalized jitter standard deviation in various atmospheric turbulence conditions.*

The outage probability dependence on $\mu_1 = \mu_2$ (balanced SNR scenario), for different values of the normalized jitter standard deviation in various atmospheric turbulence conditions is presented in Fig. 2. System has better performance when the index of refraction structure parameter is lower, meaning the conditions of atmospheric turbulence are more favorable to perform wireless optical signal transmission. As it was concluded before, smaller normalized jitter standard deviation leads to better system performance. Also, from Fig. 2 can be observed that the pointing errors effect is more pronounced and have more impact on the system performance in weak atmospheric turbulence conditions. On the other hand, when optical signal transmission suffers from

strong atmospheric turbulence, misalignment between FSO apertures has minor effect on the outage probability performance.
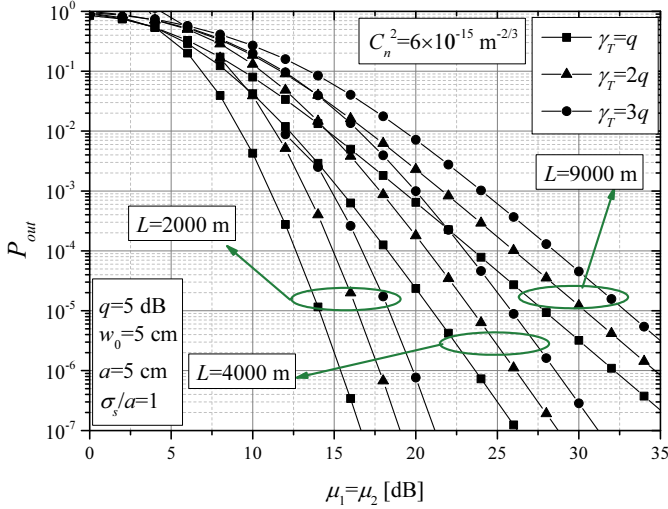

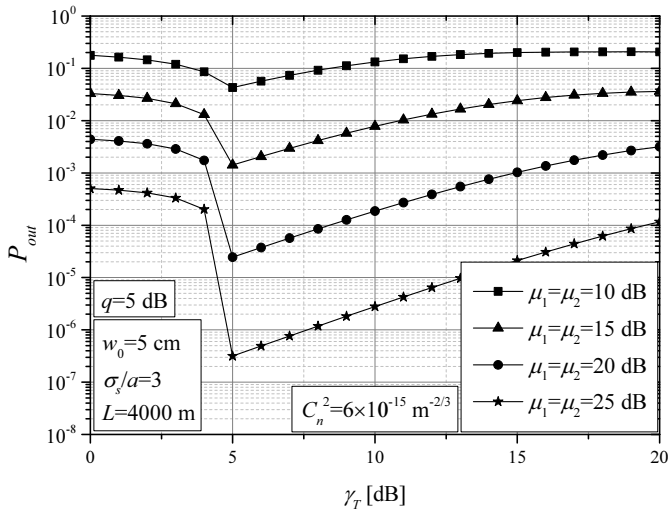**Fig. 3** – *Outage probability versus μ₁=μ₂ for different values of propagation distance.*

Fig. 4 – *Outage probability versus γ_T.*

In Fig. 3, the outage probability dependence on $\mu_1 = \mu_2$ is observed, considering different values of propagation distance. The results are obtained for different values of the switching threshold. System has better performance when the FSO link length is shorter. Regarding the switching threshold, the system has the best performance when the values of the switching threshold and outage threshold are equal.

The outage probability dependence on the switching threshold for different values of the average SNR is presented in Fig. 4. When the transmitted optical power is greater, system has better performance. We can notice that the optimal value of the switching threshold can be obtained for minimal outage probability. This optimal value of the switching threshold is equal to the value of the outage threshold, i.e., $\gamma_T = q$. In this case, the SSC receiver represents SC receiver, which gives the best outage probability performance.

5   Conclusion

In this paper, we have analyzed the coherent FSO system employing the SSC dual diversity receiver. It has been assumed that optical signal intensity fluctuations are result of the Gamma-Gamma atmospheric turbulence and the pointing errors. Novel expressions for the outage probability have been derived, considering general scenario of unbalanced average SNRs, as well as the simpler balanced SNR case when the signals at the receiver have equal powers. The impact of different system and channel parameters was observed and discussed.

It has been concluded that the SSC branch unbalancing causes significant outage probability degradation. Also, the degradation due to the unbalanced SNR is independent on the FSO channel state, such as pointing errors. Furthermore, strong atmospheric turbulence and pointing errors can cause serious performance degradation of the system. In addition, when FSO signal transmission is affected by strong atmospheric turbulence, pointing errors have negligible impact on the outage probability. It has been also concluded that the best system performance is achieved when the switching threshold value is equal to the outage threshold value, which means that the SSC receiver represents SC receiver.

6   Acknowledgement

7   References

[1]   S. Arnon, J. Barry, G. Karagiannidis, R. Schober, M. Uysal: Advanced Optical Wireless Communication Systems, Cambridge University Press, NY, USA, 2012.

[2]   L.C. Andrews, R.L. Philips: Laser Beam Propagation through Random Media, Spie Press, Bellingham, Washington, DC, USA, 2005.

[3]   Z. Ghassemlooy, W. Popoola, S. Rajbhandari: Optical Wireless Communications: System and Channel Modelling with MATLAB®, CRC Press, Taylor and Francis Group, Boca Raton, FL, USA, 2012.

[4]   M.A. Khalighi, M. Uysal: Survey on Free Space Optical Communication: A Communication Theory Perspective, IEEE Communications Surveys and Tutorials, Vol. 16, No. 4, Fourthquarter 2014, pp. 2231 – 2258.

[5]   A.A. Farid, S. Hranilovic: Outage Capacity Optimization for Free-space Optical Links with Pointing Errors, Journal of Lightwave Technology, Vol. 25, No. 7, July 2007, pp. 1702 – 1710.

[6]   H.G. Sandalidis: Optimization Models for Misalignment Fading Mitigation in Optical Wireless Links, IEEE Communications Letters, Vol. 12, No. 5, May 2008, pp. 395 – 397.

[7]   H.G. Sandalidis, T.A. Tsiftsis, G.K. Karagiannidis: Optical Wireless Communications with Heterodyne Detection over Turbulence Channels with Pointing Errors, Journal of Lightwave Technology, Vol. 27, No. 20, Oct. 2009, pp. 4440 – 4445.

[8]   A. Farid, S. Hranilovic: Outage Capacity for MISO Intensity-modulated Free-space Optical Links with Misalignment, IEEE/OSA Journal of Optical Communications and Networking, Vol. 3, No. 10, Oct. 2011, pp. 780 – 789.

[9]   S. Arnon: Effects of Atmospheric Turbulence and Building Sway on Optical Wireless-communication Systems, Optics Letters, Vol. 28, No. 2, Jan. 2003, pp. 129 – 131.

[10] W.O. Popoola, Z. Ghassemlooy, J.I.H. Allen, E. Leitgeb, S. Gao: Free-space Optical Communication Employing Subcarrier Modulation and Spatial Diversity in Atmospheric Turbulence Channel, IET Optoelectronics, Vol. 2, No. 1, Feb. 2008, pp. 16 – 23.

[11] T.A. Tsiftsis, H.G. Sandalidis, G.K. Karagiannidis, M. Uysal: Optical Wireless Links with Spatial Diversity over Strong Atmospheric Turbulence Channels, IEEE Transactions on Wireless Communications, Vol. 8, No. 2, Feb. 2009, pp. 951 – 957.

[12] E. Bayaki, R. Schober, R.K. Mallik: Performance Analysis of MIMO Free-space Optical Systems in Gamma-Gamma Fading, IEEE Transactions on Communications, Vol. 57, No. 11, Nov. 2009, pp. 3415 – 3424.

[13] X. Lei, D. Xiaodai: New Results on the BER of Switched Diversity Combining over Nakagami Fading Channels, IEEE Communications Letters, Vol. 9, No. 2, Feb. 2005, pp. 136 – 138.

[14] H. Moradi, H.H. Refai, P.G. Lopresti: Switch-and-stay and Switch-and-examine Dual Diversity for High-speed Free-space Optics Links, IET Optoelectronics, Vol. 6, No. 1, Feb. 2012, pp. 34 – 42.

[15] M.I. Petkovic, G.T. Djordjevic: Outage Performance of SSC Receiver in FSO System with Gamma-Gamma Atmospheric Turbulence, XII International SAUM Conference on Systems, Automatic Control and Measurements, Nis, Serbia, 12-14 Nov. 2014, pp. 324 – 327.

[16] M.I. Petkovic, G.T. Djordjevic: Impact of Pointing Errors on the Outage Probability Performance of the FSO System with SSC Receiver, ETRAN Conference, Zlatibor, Serbia, 13-16 June 2016, p. TE2.3. (In Serbian).

[17] M. Niu, J. Cheng, J.F. Holzman: Error Rate Performance Comparison of Coherent and Subcarrier Intensity Modulated Optical Wireless Communications, IEEE/OSA Journal of Optical Communications and Networking, Vol. 5, No. 6, June 2013, pp. 554 – 564.

[18] I.S. Gradshteyn, I.M. Ryzhik: Table of Integrals, Series and Products, Academic Press, NY, USA, 2000.

[19] The Wolfarm Functions Site, 2008. Available at: http:/functions.wolfram.com.

[20] E. Zedini, I.S. Ansari, M.S. Alouini: Unified Performance Analysis of Mixed Line of Sight RF-FSO Fixed Gain Dual-hop Transmission Systems, IEEE Wireless Communications and Networking Conference, New Orleans, LA, USA, 09-12 March 2015, pp. 46 – 51.

[21] M.K. Simon, M.S. Alouni: Digital Communication over Fading Channels, John Wiley and Sons, NY, USA, 2004.